Structural Engineering and Mechanics, Vol. 45, No.1 (2013) 129 - 144

DOI: http://dx.doi.org/10.12989/sem.2013.45.1.129

Theoretical and experimental study on load-carrying capacity of combined members consisted of inner and sleeved tubes

Bo Hu[a], Boqing Gao[*], Shulin Zhan[b] and Cheng Zhang[c]

College of Civil Engineering and Architecture, Zhejiang University, Hangzhou 310058, China

(Received August 19, 2012, Revised October 31, 2012, Accepted December 1, 2012)

Abstract. Load-carrying capacity of combined members consisted of inner and sleeved tubes subjected to axial compression was investigated in this paper. Considering the initial bending of the inner tube and perfect elasto-plasticity material model, structural behavior of the sleeved member was analyzed by theoretic deduction, which could be divided into three states: the elastic inner tube contacts the outer sleeved tube, only the inner tube becomes plastic and both the inner and outer sleeved tubes become plastic. Curves between axial compressive loads and lateral displacements of the middle sections of the inner tubes were obtained. Then four sleeved members were analyzed through FEM, and the numerical results were consistent with the theoretic formulas. Finally, experiments of full-scale sleeved members were performed. The results obtained from the theoretical analysis were verified against experimental results. The compressive load-lateral displacement curves from the theoretical analysis and the tests are similar and well indicate the point when the inner tube contacts the sleeved tube. Load-carrying capacity of the inner tube can be improved due to the sleeved tube. This paper provides theoretical basis for application of the sleeved members in reinforcement engineering.

Keywords: sleeved member; axial compressive load; load-carrying capacity; numerical analysis; experimental study

1. Introduction

The instability of compressive steel members is one of the most important issues that should be considered in the process of design and construction of a steel structure (Cai *et al.* 2012). Many researchers have carried out investigations for the analysis approaches of stability of steel members (Kwak *et al.* 2003, Serna *et al.* 2011). Compressive steel members with large slenderness ratio are prone to buckling and losing load-carrying capacity, thus causing severe threats to structural security (Siginer 1992, Marques *et al.* 2009, Barakat 2011). Grid structures carry their loads mainly by compression forces, so the stability problem play an important role within the analysis of these structures (Bulenda and Knippers 2001 and Rahman 2010), and the buckling instability of compressive members may lead to the failure of the whole structure (Gosowski 2003,

*Corresponding author, Professor, E-mail: bqgao@zju.edu.cn
[a]Master Candidate, E-mail: hubo@zju.edu.cn
[b]Professor, E-mail: jzcl@zju.edu.cn
[c]PhD Candidate, E-mail: c-zhang@zju.edu.cn

He and Zhou 2011). Therefore, if the bucking is restrained by corresponding reinforcement measures like sleeved members, the load-carrying capacity of compressive members and furthermore the performance of the structure could be improved.

Since sleeved members were proposed in 1990, related scholars have made more in-depth study on the behavior of sleeved member. The sleeved member is composed of an inner core and an outer component, and with gap between them. The inner core bears the axial compression, while the outer component restrains the inner core from buckling and improves its post-buckling behavior, thereby enhancing its load-carrying capacity (Sridhara 1993). Prasad (1992) did pressure experiments for reduced scale sleeved members, whose outer components stiffness was infinite, and obtained the curves between axial loads and axial displacements of inner cores. Chin (1998) analysed the post-buckling behavior of linearly elastic columns between two rigid guiding walls, declaring that the linearly elastic column may have local instability problem which consequently leads to the instantaneous transition of its buckling waveform to a new equilibrium configuration, and he verified the results through experiments. According to the criterion that the horizontal deflection would tend to infinity when the member is instable, Sridhara (1993) deduced the deflection calculation formula of the inner core under axial compression when the stiffness of the outer component was finite, and discussed the influence of stiffness ratio of the inner and outer components on load-carrying capacity of the inner core, finally put forward that high order mode buckling can emerge in the inner core while the stiffness of the outer was large enough; Shen and Deng (2007) improved the details of the sleeved member: inner cores and outer components were steel tubes, and restraint- location connections were used at the ends of the inner tube. They proposed a mechanical model of line contact between the two tubes, then made behavior analysis on the contact of the inner and outer tubes within linear elastic range, and obtained calculation formulas of deflection, moment, shear etc. of the inner tube. However, they failed to consider the condition that the inner tube went into plastic. As the axial compressive load increases, the performance of the inner tube needs further analysis after the inner tube being plastic. Furthermore, in the existing structure, the outer tubes are unable to be added to the inner tubes to form sleeved members using the existing form of sleeved members, so this kind of sleeved members is difficult to achieve in practical application.

To solve these problems, this paper intended to improve the details of the sleeved member at first. Then the load-carrying capacity of the sleeved member under axial compression was studied, considering the initial bending of the inner tube. Full-scale model loading experiments were conducted to verify the results from the theoretical analysis. This paper can provide theoretical basis for the application of sleeved members in reinforcement engineering.

2. Details of sleeved members

Fig. 1 describes the details of commonly used sleeved members at present. To ensure that the inner tube bears the whole axial force, the outer tube is slightly shorter than the inner. But we can still presume that they have the same effective length during the theoretical analysis. Connections between the inner tube and other members in a structure are supposed to be hinge jionts, and the ends of the outer tube are connected with the inner tube using the restraint-location connections like the contact-rings, so as to make the outer tube simultaneously offset with the inner before both of the middle sections contact. The connection is similar to an active articulated structure (Shen and Deng 2007), because it does not transfer the axial force, and allows the relative rotation of the inner tube and the outer.

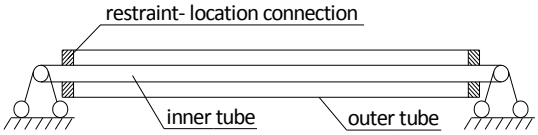

Fig. 1 Former sleeved members

In order to facilitate the installation of outer sleeved tubes on the existing members, this paper improved the details of the sleeved member. As shown in Fig. 2, the outer tube comprises two semi-circular and constant-section steel tubes with ear-plate connections, which are only set at both ends and the middle of the outer tube. The steel tubes are connected together by bolts.

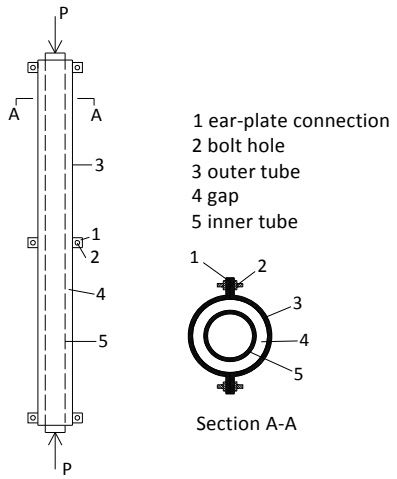

Fig. 2 Details of the improved sleeved member

3. Structural behavior of sleeved members under axial compression

From the research of Domokos *et al.* (1997), when the inner tube transits from the lowest order buckling mode to the second order buckling mode under axial compression, the value of axial compression would be 15.875 times the Euler load. It should be mentioned that large plastic deformation will be bound to arise in the inner tube and the outer tube with finite stiffness under this huge axial force. It is assumed the sleeved members be wrecked when the stress on the edge of the middle section of outer tube reaches the yield stress. Therefore, in the analysis of mechanical behavior of the sleeved members, the inner and outer tubes keep single point contact with each other after the instable inner tube contact the outer one, and the inner tube can not be in a high order buckling mode or line contact with the outer tube. This process consists of three stages that the inner and outer tubes are in contact in the elastic state, the inner tube goes into the plastic state and both of them become plastic, and the corresponding axial loads are P_1, P_2, P_3, respectively. Basic assumptions in the analysis process are as following: the inner and outer tubes are perfect elasto-plasticity material members, the plane cross-section of members remains plane after bending, the deformation is small, and the tangential friction force between the inner and outer tubes is ignored.

Using the basic details of the sleeved member and related assumptions, the analysis sketch is shown in Fig. 3. Because the thickness of the inner tube is less than 1/15 ~ 1/20 of the diameter of the tube in general, the inner tube belongs to thin-walled members, so the area of the inner tube can be concentrated in the center axis of the wall-thickness of the tube, and similar simplification can be made to the modulus and moment of inertia of cross-section of the inner tube.

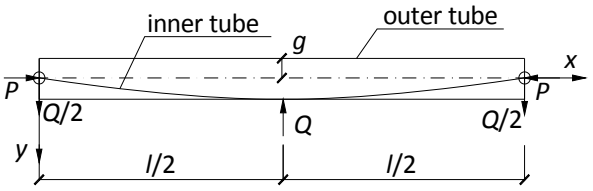

Fig. 3 Analysis sketch of a sleeved member

3.1 Stage I

Initial bending, which is the same as the first order buckling mode of the inner tube, is considered in the inner tube. The initial deflections of the points of the inner tube are defined by $y_0=v\sin(\pi x/l)$, where l is the effective length, v is the initial deflection of the middle section, which is valued $l/1000$. We establish the equilibrium equation for the inner tube

$$EI(y''-y_0'')+Py=0 \tag{1}$$

where E is the elastic modulus, I is the section inertia moment of the inner tube, P is the axial compressive load, and y is the lateral deflection of the inner tube.

Considering the boundary conditions, the equation of the deflection curve of the inner tube is obtained

$$y=\frac{1}{1-P/P_E}v\sin\frac{\pi x}{l} \tag{2}$$

where P_E is the Euler load of the inner tube, and $P_E=\pi^2EI/l^2$.

D and d respectively represent the external diameters of the outer and inner tubes, and the thickness of tubes are respectively T and t; so the gap between the two tubes $g = (D-d)/2-T$. The inner and outer tubes will be in contact when the lateral displacement of the middle section of the inner tube δ reaches to g, the point (P_1, δ_1) on the curve between the axial compressive load and the lateral displacement of the middle section of the inner tube (P-δ curve) is obtained, where axial compression $P_1= (1-v/g)P_E$. After the contact, the tubes squeeze each other at the contact point, and a concentrated contact force Q is produced. Then the equilibrium equation of the inner tube is established again

$$EI(y''-y_0'')+Py=Qx/2 \tag{3}$$

Also, considering the boundary conditions, we obtain the new equation of the deflection curve of the inner tube

$$y=-\frac{Q}{2kP}\sec\frac{kl}{2}\sin kx+\frac{Qx}{2P}+\frac{1}{1-P/P_E}v\sin\frac{\pi x}{l} \tag{4}$$

where $k^2=P/EI$, so the lateral deflection of the middle section of the inner tube is

$$\delta=y(\frac{l}{2})=\frac{Q}{2kP}(\frac{kl}{2}-\tan\frac{kl}{2})+\frac{v}{1-P/P_E} \tag{5}$$

The outer tube is elastic in this stage, and bears a concentrated load at its middle section, so the middle section lateral deflection $\delta_e = Ql^3/48EI_e$, where I_e is the section inertia moment of the outer tube. Then combining $g=\delta-\delta_e$ with Eq. (5), we eliminate Q and get

$$\delta=\frac{24EI_eg(\frac{kl}{2}-\tan\frac{kl}{2})-\frac{vkPl^3}{1-P/P_E}}{24EI_e(\frac{kl}{2}-\tan\frac{kl}{2})-kPl^3} \tag{6}$$

According to Eq. (6), the relationship between P and δ is obtained in this stage. When the axial compression continues to increase, the stress at the edge of the middle section of the inner tube reaches to the yield stress f_y

$$\frac{P}{A}+\frac{M}{W}=\frac{P}{\pi dt}+\frac{P\delta-Ql/4}{\pi d^2t/4}=f_y \tag{7}$$

where A and W are respectively the area and modulus of cross-section of the inner tube.
From the deflection relationship formulas of the middle sections of the inner and outer tubes, the following equation is obtained

$$Ql=\frac{48EI_e(\delta-g)}{l^2} \tag{8}$$

Substituting Eq. (8) into Eq. (7), we can get

$$\delta=\frac{Pd+48EI_eg/l^2-\pi d^2tf_y}{48EI_e/l^2-4P} \tag{9}$$

Through Eq. (6) and Eq. (9), we can solve for P_2 and the corresponding lateral deflection δ_2, so we get the point (P_2, δ_2) on the P-δ curve.

3.2 Stage II

With the increase of the axial load, part of the middle section of the inner tube goes into plastic. Fig. 4 exhibits the stress and strain of the middle section of the inner tube. Shaded area represents the plastic zone, and the height of elastic region h_e is equal to $(1+\cos\alpha_0)d/2$, where $\alpha_0\in(0,\ \pi)$.

Equation of the axial force balance is

$$P=P_y-\frac{dt(\sigma_y+\sigma_t)[(\pi-\alpha_0)\cos\alpha_0+\sin\alpha_0]}{1+\cos\alpha_0} \tag{10}$$

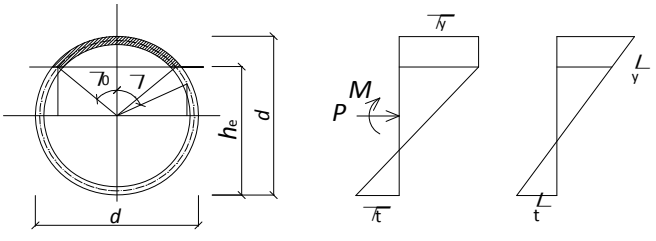

(a) middle section (b) stress (c) strain

Fig. 4 Stress and strain of the middle section of the inner tube

where P_y is the axial compressive load when the middle section of the inner tube is completely plastic.

The moment equilibrium equation is

$$P\delta - \frac{Ql}{4} = \frac{d^2 t(\sigma_y + \sigma_t)[(\pi - \alpha_0) + \sin\alpha_0 \cos\alpha_0]}{4(1+\cos\alpha_0)} \tag{11}$$

From Fig. 4, the curvature of the middle section of the inner tube is

$$\Psi = \frac{\varepsilon_y + \varepsilon_t}{h_e} = \frac{\sigma_y + \sigma_t}{Eh_e} = \frac{2(\sigma_y + \sigma_t)}{Ed(1+\cos\alpha_0)} \tag{12}$$

Due to the shape of deformation and boundary conditions, we can assume that the equation of inner tube deflection curve is: $y=\delta\sin(\pi x/l)$, and the curvature is $-y''$. Before loading, the initial deflection equation of the inner tube is: $y_0=v\sin(\pi x/l)$, and the curvature is $-y_0''$. So the curvature which is corresponding to the internal moment of the middle section is

$$\Psi = [-y''(\frac{l}{2})] - [-y_0''(\frac{l}{2})] = \frac{(\delta - v)\pi^2}{l^2} \tag{13}$$

Associating with Eq. (10), Eq. (12) and Eq. (13), we can get

$$\delta = \frac{2(P_y - P)l^2}{\pi^2 Ed^2 t[(\pi - \alpha_0)\cos\alpha_0 + \sin\alpha_0]} + v \tag{14}$$

Also, associating with Eq. (10), Eq. (11), Eq. (12) and Eq. (13), we can get

$$\frac{P_y - P}{dt} - \frac{(4P\delta - Ql)\cos\alpha_0}{d^2 t} = \frac{Ed\sin^3\alpha_0(\delta - v)\pi^2}{2l^2} \tag{15}$$

The Eq. (8) is still applicable to the outer tube in the elastic state, and is substituted into the Eq. (15), the following equation is obtained

$$\delta = \frac{48EI_e g\cos\alpha_0 / l^2 - (P_y - P)d - E\pi^2 vd^3 t\sin^3\alpha_0 / 2l^2}{48EI_e\cos\alpha_0 / l^2 - E\pi^2 d^3 t\sin^3\alpha_0 / 2l^2 - 4P\cos\alpha_0} \tag{16}$$

Let α_0 be (0, π), and then we can obtain a series of points on the P-δ curve from Eq. (14) and Eq. (16).

When α_0 is equal to 0, Eq. (16) is equivalent to Eq. (9), so the above P_2 and δ_2 satisfy Eq. (16), which indicates that the P-δ curve is continuous at the point (P_2, δ_2).

When α_0 is equal to π, the middle section of the inner tube is completely plastic. We can get these equations: $P_2' = P_y$, $P_2'\delta_2' = Ql/4 = 12EI_e(\delta_2'-g)/l^2$. And the point ($P_2'$, δ_2') is obtained from them.

3.3 Stage III

Since inner tube is elastic-perfectly plastic material, the stress of the middle section remains f_y, and still satisfies $P\delta = Ql/4$ after it being completely plastic. The outer tube has not yet entered into

plasticity, which means that the stress at the edge of the middle section of the outer tube has not yet reached the yield stress, so δ still satisfies the following equation

$$\delta = \frac{12EI_e g}{12EI_e - Pl^2} \tag{17}$$

The outer tube also begins to go to plastic when (Ql /4) / ($2I_e/D$) is equal to f_y, we can get

$$P = \frac{12f_y EI_e}{6EDg + f_y l^2} \tag{18}$$

Substituting the equation $g = (D\text{-}d)/2\text{-}T$ into Eq. (18), we get the further calculation formula

$$P = \frac{12f_y EI_e}{3ED(D-d) - 6EDT + f_y l^2} \tag{19}$$

P_3 and δ_3 can be solved through Eq. (19) and Eq. (17), then the point (P_3, δ_3) on the P-δ curve is obtained. And P_3 is the failure axial compressive load for the sleeved member.

4. Numerical examples

Three groups of sleeved members were selected. Group 1: the sections of outer tubes were all Φ89 × 4 in mm, the sections of inner tubes were Φ45 × 3, Φ48 × 3, Φ54 × 3, Φ57 × 3, Φ60 × 3.5, respectively, and the lengths of members were all 2500 mm. Group 2: the sections of inner tubes were all Φ48 × 3, the sections of outer tubes were Φ68 × 3.5, Φ73 × 4, Φ76 × 4, Φ83 × 4, Φ89 × 4, respectively, and the lengths of members were all 250 0mm. Group 3: the sections of the inner were all Φ48 × 3, that of outer tubes were all Φ76 × 4, and the lengths of members were 1800 mm, 2000 mm, 2200 mm, 2500 mm, 2800 mm, 3000 mm, respectively. According to the formulas in the above derivation, the P-δ curves of all selected sleeved members were obtained by using MATLAB software.

Fig. 5 shows the P-δ curves of sleeved members in three groups. The first inflection point on the curve is corresponding to the time when the inner tube contacts with the outer at the middle section. After the first inflection point, the outer tube begins to play the role of lateral restraint so that the lateral stiffness of the inner tube increases. The second inflection point is corresponding to the time when the middle section of the inner tube is completely plastic, and the axial compressive load at this time is the yielding load of the inner tube. The middle section of the inner tube becomes a plastic hinge and the contact force keeps the bending moment consistent. Therefore, we can approximate that the lateral stiffness of the inner tube increases again. The outer tube can play the role of lateral support for the inner tube after being in contact with it, and the failure mode of the inner tube is yielding but not buckling. Thereby the load-carrying capacity of the inner tube increases and even more than its yielding load. From Fig. 5(a), we can find that with the sizes of

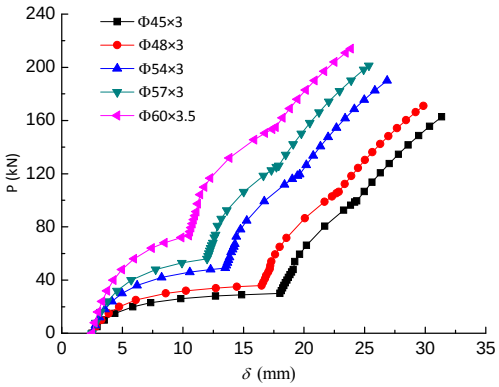

(a) *P*-*δ* curves of the same outer tube and different inner tubes

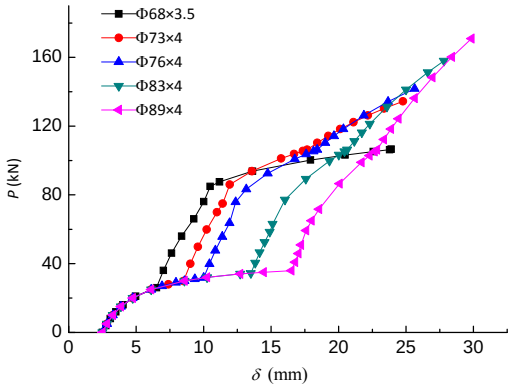

(b) *P*-*δ* curves of the same inner tube and different outer tubes

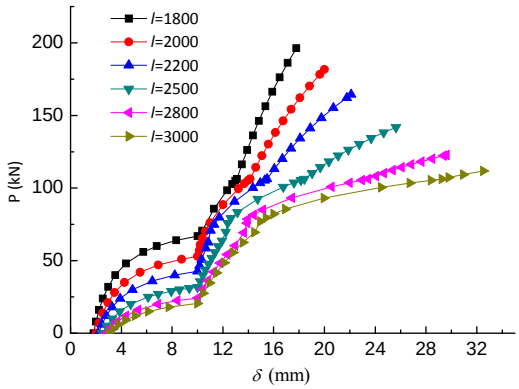

(c) *P*-*δ* curves of the same section and different lengths

Fig. 5 *P*-*δ* curves of sleeved members

the outer tubes unchanged, the failure load of the sleeved member increases with the increasing of the stiffness of the inner tube. From Fig. 5(b), we can see that with the sizes of the inner tubes unchanged, the failure load of the sleeved member increases with the increasing of the stiffness of the outer tube. From Fig. 5(c), we know that the larger the slenderness ratio of the inner tube, the greater the ratio of the failure load to the Euler load, and the more improvement the load-carrying capacity of the inner tube. For sleeved members whose slenderness ratios are relatively small, the edge of the middle section of the inner tube may be plastic before the inner tube and the outer being in contact, the contact force constraints the development of the plastic region of the inner tube, and gradually counteracts the negative stiffness which comes from the axial compression. Even though the inner tube comes into plastic state, the theoretical analysis still works. As a result, the ultimate failure mode and calculation formula of the failure load of the sleeved member remain unchanged.

5. Finite element analysis

Sleeved members were simulated and analyzed by using finite element software ANSYS. The three-dimensional beam188 element was selected for the inner tube, the lowest order buckling mode of the inner was chosen as its initial deformation distribution, and the solid45 element was used for the outer tube. The combin 39 nonlinear spring element was chosen for simulating the contaction of the inner and outer tubes. There were two kinds of the inner tube sections: Φ48 × 3, Φ60 × 3.5 and two kinds of the outer tube sections: Φ76 × 4, Φ89 × 4, the lengths of members were all 2500 in mm, so we got four choices of sleeved members through their combinations: (1) the inner tube section was Φ48 × 3, that of the outer was Φ76 × 4; (2) the inner tube section was Φ48 × 3, that of the outer was Φ89 × 4; (3) the inner tube section was Φ60 × 3.5, that of the outer was Φ76 × 4; (4) the inner tube section was Φ60 × 3.5, and the outer tube section was Φ89 × 4. The *P*-*δ* curves were also obtained by finite element analysis. Taking into account the simplification of section properties of the thin-walled inner tube during the theoretic analysis, the axial pressure load of analytical solution should be multiplied by the corresponding reduction coefficient while compared with ANSYS numerical solution. The reduction coefficient was the stiffness ratio of the inner tube section before and after the simplification. Furthermore, the lateral displacement became a mutation after forming a plastic hinge in middle section of the inner tube in numerical analysis, so part of the *P*-*δ* curves from formula derivation and numerical analysis are compared.

As shown in Fig. 6, the two curves of four sleeved members are consistent approximately, which verifies the rationality of theoretical derivation and the above assumptions. The part of curve before the inflection point describes that the inner tube loses lateral stiffness gradually under the axial compression, and that the slope of the curve decreases. The part of curve after the inflection point exhibits that the outer tube constraints the lateral deformation of the inner tube and provides lateral stiffness for it with they being contact, which thereby increases the load-carrying capacity of the inner tube.

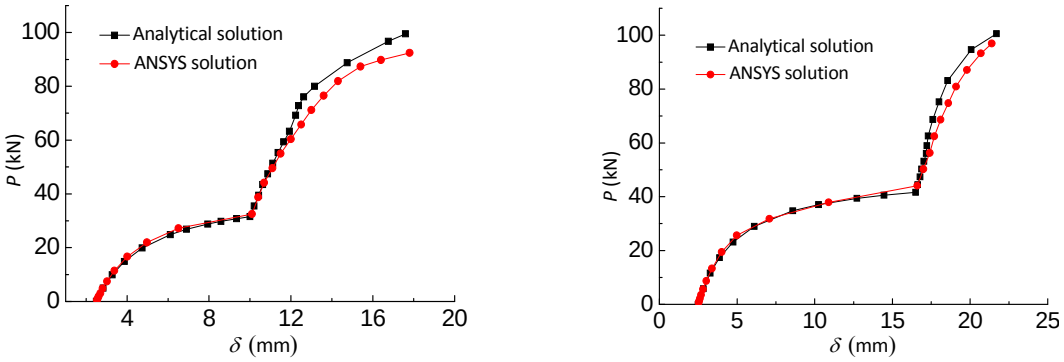

(a) *P*-*δ* curves of (1) (b) *P*-*δ* curves of (2)

Fig. 6 *P*-*δ* curves of four sleeved members

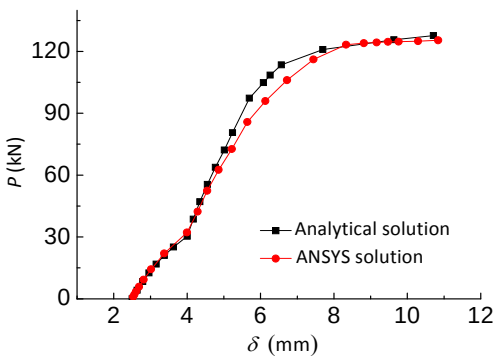

(c) P-δ curves of (3)

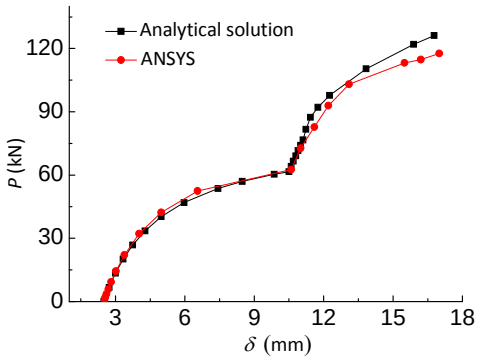

(d) P-δ curves of (4)

Fig. 6 Continued

6. Experimental verification

6.1 Specimen Selection

Four sleeved members of different sizes and two single steel tubes, which have the same section with the inner tube, were selected in this experiment. So there were six experiment specimens in total. Table 1 summarizes the information about the specimens selected to be tested.

Table 1 Size and material of the specimens

	Outside diameters (mm)	Thickness (mm)	Length (mm)	Material
Inner tube	48	3	2600	Q235
	60	3.5	2600	Q235
Outer tube	76	4	2500	Q235
	89	4	2500	Q235

Fig. 7 shows the specimen of the sleeved member: the inner tube and the end plate are connected by welding and the stiffening ribs are setting in the end, so the connection can be assumed rigid. And the end plate is perpendicular to the inner tube. The outer tube is made up of two semi-circular steel tubes with constant-section. The two steel tubes are assembled through six pairs of ear-plates, which are fixed at both ends and middle of the steel tubes. Weld is also used for the connection of ear-plates and the outer tube. The axial compressive load was applied to the end plate.

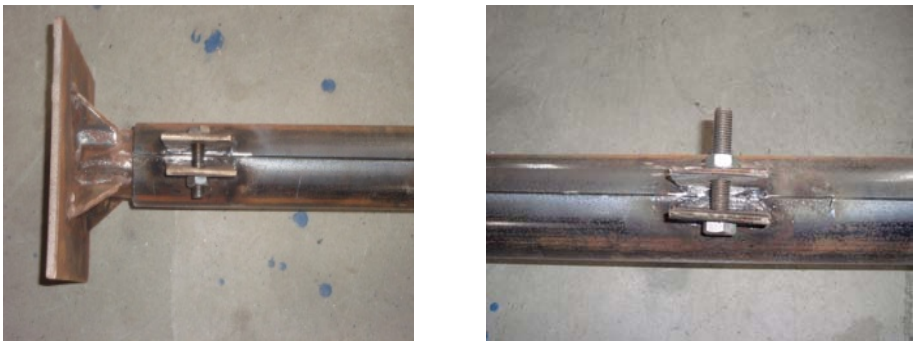

(a) the end of sleeved member (b) the middle part of sleeved mamber

Fig. 7 Specimen of the sleeved member

6.2 Test Setup and the Loading Scheme

Uni-axial compression tests are performed by a 300 kN jack. The test setup consists of a hydraulic jack, a force sensor, displacement sensors, data acquisitions, test specimens, etc. As shown in Fig. 8, the experiment rack is a self-balanced force system with a large counter-force beam, which is 3200 in mm above the ground. The load was exerted along the vertical direction. This test used pressure-control loading method, and applied step loading according to the estimated load-carrying capacity of specimens. The lateral displacement of the middle section of the inner tube was measured through two displacement sensors, which were installed horizontally in two orthogonal direction of the inner tube middle section before loading.

(a) Loading pedestal (b) Experiment rack

Fig. 8 Photos of the loading equipment

6.3 Main Results and Analysis

During the process of loading, the axial compression loads were treated as the load-carrying capacity of specimens in the experiment, if which stopped increasing and kept constant. The load-carrying capacity of six specimens was obtained in this experiment. As shown in Table 2, the load-carrying capacity of the sleeved member is larger than that of the single tube, which has the same section with the inner tube, and it increases with the increasing of the stiffness of the outer tube. In addition, the deformation conditions of specimens after loading were shown in Fig. 9, the lateral deformation of the sleeved member was obviously less than that of the single steel tube.

Table 2 Load-carrying capacities of members (Unit: kN)

	Single tube	Φ76 × 4 outer tube	Φ89 × 4 outer tube
Φ48×3	62.9	100.9	103.9
Φ60×3.5	83.6	127.9	146.6

(a) Sleeved member (b) Single tube

Fig. 9 Status of the members after experiment

As shown in Fig. 10, *P-δ* curves from the experiments and the theoretical analysis are compared. The load-carrying capacity from the tests is slightly larger than the theoretical analysis. The increased strength can be attributed to the following factors: 1) the ends of loading devices are not ideal hinge joints; 2) the initial imperfections of specimens are not well distributed; 3) the hardening segment due to the specimen manufacturing. But the axial compressive loads-lateral displacements curves from the theoretical analysis and the tests are

similar and more importantly, the infection points which indicate the moment when the inner tube contacts the sleeved tube can be obtained. It well demonstrates the effectiveness of the sleeved member details proposed in the papers and the reliability of the theoretical analysis.

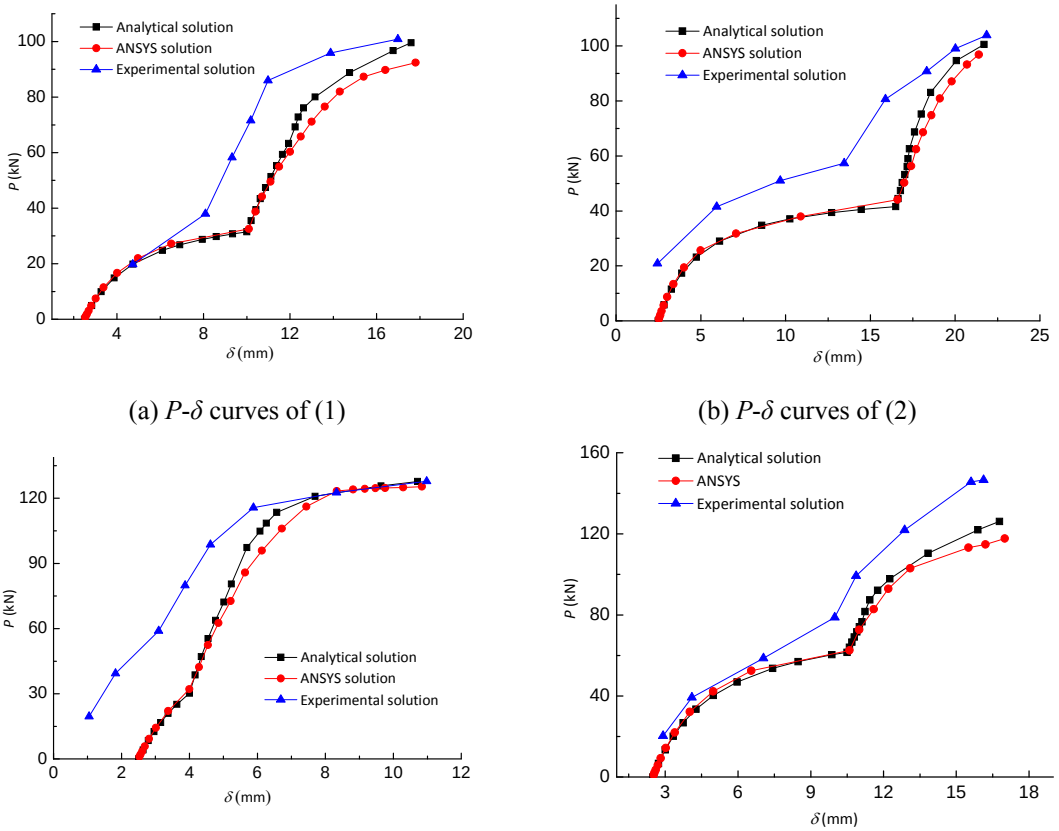

(a) P-δ curves of (1)

(b) P-δ curves of (2)

(c) P-δ curves of (3)

(d) P-δ curves of (4)

Fig. 10 P—δ curves of four sleeved members

7. Conclusions

In this paper, we improved the details of the sleeved member by using two semi-circular and constant-section steel tubes instead of a seamless circular tube, and setting ear-plate connections at the ends and middle of the steel tubes, each pair of ear-plates is linked by bolts. Then aiming at sleeved members under the axial compression and considering the initial bending of inner tubes, the curves and equations of the whole loading process between the lateral displacement of the inner tube middle section and the axial compressive load were derived, using the second-order

equilibrium equations of small deflection and the plastic theory of press-bend member. Then the curves were verified by finite element analysis and experimental studies. Finally, we can get the following conclusions:

(1) Due to the lateral support of the outer tube, the stability problem of the inner tube changes into intensity problem, thus load-carrying capacity of the inner tube is improved. The load-carrying capacity of the sleeved member increases with the increasing of the stiffness of the outer tube if the sizes of the inner tubes are constant. The load-carrying capacity of the sleeved member increases with the increasing of the stiffness of the inner tube if the sizes of the inner tubes are constant.

(2) The larger slenderness ratio of the inner tube, the more improvement of load-carrying capacity of the inner tube after forming sleeved member. For sleeved members whose slenderness ratios are relatively small, the edge of the middle section of the inner tube may be plastic before the inner tube and the outer contact, but the ultimate failure mode and ultimate design formulae of the sleeved member remain unchanged.

(3) Comparing the theoretical analysis results with the experimental results, the inflection point and the trends of the P-δ curves are all consistent, which verifies the rationality of the improved structure model of the sleeved member and the theoretical analysis. The result obtained in this paper provides the theoretical basis for application of the sleeve members in reinforcement engineering.

Acknowledgments

This work described in paper was supported by the National Natural Science Foundation of China (No. 51178414) and Science Foundation of Zhejiang Province (No. Y1110438).

References

Barakat, S. (2011), "Experimental compression tests on the stability of structural steel tabular props", *Jordan Journal of Civil Engineering*, **5**(1), 107-117.

Bulenda, Th. and Knippers, J. (2001), "Stability of grid shells", *Computer & Structures*., **79**, 1161-1174.

Cai, J.G., Xu, Y.X., Feng, J. *et al.*. (2012), "Buckling and post-buckling of rotationally restrained columns with imperfections", *Sci China-Phys Mech Astron*., **55**(8), 1519-1522.

Chai, H. (1998), "The post-buckling response of a bi-laterally constrained column", *Journal of the Mechanics and Physics of Solids.*, **46**(7), 1155-1181.

Domokos, G., Holmes, P., Royce, B. (1997), "Constrained Euler buckling". *Journal of Nonlinear Science*, **7**(3), 281-314.

Gosowski, B. (2003), "Spatial stability of braced thin-walled members of steel structures", *Journal of Constructional Steel Research*, **59**, 839-865.

He, Y.J. and Zhou, X.H. (2011), "Formation of the spherical reticulated mega-structure and its stabilities in construction", *Thin-Walled Structures*, **49**,1151-1159.

Kwak, H.G., Kim, D.Y. and Lee, H.W. (2001), "Effect of warping in geometric nonlinear analysis of spatial beams", *Journal of Constructional Steel Research*, **57**(7), 729-751.

Marques, L., Simdes da Silva L., Rebelo, C. (2009), "Application of the general method for the evaluation of the stability resistance of non-uniform members", *Proceedings of ICASS*, Hong Kong, 16-18 December.

Prasad, B.K. (1992), "Experimental investigation of sleeved column", *The 33rd AIAA/ASCE structures, structural dynamics and materials conference*, *AIAA/ASCE*, Dallas, USA.

Rahman, T. and Jansen, E.L. (2010), "Finite element based coupled mode initial post-buckling analysis of a composite cylindrical shell", *Thin-Walled Structures*, **48**(1),25-32.

Serna, M.A., Ibanez, J.R., Lopez, A. (2011), "Elastic flexural buckling of non-uniform members: Closed-form expression and equivalent load approach", *Journal of Constructional Steel Research*, **67**, 1078-1085.

Shen, B. and Deng, C.G. (2007), "Continuous transition from point contact to line contact between the axially compressed inner core and the flexible sleeve in a sleeved column", *Engineering Mechanics*, **24**(2), 154~160. (in Chinese)

Siginer A. (1992), "Buckling of columns of variable flexural rigidity", *Journal of Engineering Mechanics*, **118**, 640-643.

Sridhara, B.N. (1993), "Sleeved compression member", *patent*, USA.